Tunnelling Past Critical Structures in Kuala Lumpur: Insights from Finite Element Analysis and T-Z Load Transfer Analyses

C.W. Boon[1] and L.H. Ooi[2]
[1,2]*MMC-Gamuda KVMRT (T) Sdn Bhd*
E-mail: cwboon@kvmrt-ug.com.my

ABSTRACT: The contribution of this paper is the discussion of three case histories of tunnelling past critical structures. The first case history is on a 15-storey tower building seated on a raft foundation. The analyses provide insight with regard to the need to adapt the TBM operating performance, as the presence of the building is found to be capable of inducing larger volume loss. The second case history is on a flyover bridge, of which the pile toes are at an elevation higher than the tunnel crown. In the third case history, the piles of a Light Rail Transit (LRT) bridge were in the way of the tunnel. The piles had to be removed and underpinned with new piles which terminate below the tunnel invert. For these two case histories, we demonstrate the use of the load transfer t-z and Q-z method (Seed & Reese, 1967), which can be implemented easily into a spreadsheet, to estimate the pile settlements induced by tunnelling. The load transfers on the piles were found to be affected by (i) the soil settlement trend, which could be either increasing or decreasing with depth, and (ii) the shaft and end-bearing stiffness. The potential influences of (i) a soft base for bored piles and (ii) pile groups are discussed. Finally, insights obtained from the t-z and Q-z analyses are used to derive the influence zones due to tunnelling, and they show similar trends to the influence zones previously proposed by Jacobsz et al. (2004) derived from centrifuge tests. The line joining the points of inflection of multiple subsurface Gaussian settlement profiles (Mair et al., 1993) at different depths was found to define the boundary at which the trend of soil settlement changes from increasing with depth to decreasing with depth.

Keywords: Tunnelling induced settlements, Face pressure, T-Z method, Load transfer method, Influence Zone

1. INTRODUCTION

As MRT lines are constructed in densely populated and built-up urban areas to fulfil the need for better transportation, at least some sections of the MRT lines will inevitably have to be constructed underground. The Klang Valley Mass Rapid Transit Sungai Buloh-Kajang (KVMRT-SBK) Line is the first MRT project in Malaysia with an underground section of approximately 9.3 km in length. The geotechnical considerations for tunnelling works and protection of structures were critical to the success of this project.

One of the challenges in a tunnelling project is to minimise potential impacts to existing structures. Nearby structures which could be impacted by tunnelling have to be identified, and if the risks are found to be substantial, protection measures have to be undertaken to ensure the safety of the structures. In the KVMRT project, the twin tunnels with internal diameters of 5.8 m have to encroach into the vicinity of important historical buildings and critical structures such as flyovers, bridge piers, Light Rail Transit (LRT) viaduct piers and stations in Kuala Lumpur. The assessment of tunnelling impact to these structures and the protection measures, which had been undertaken in this project, led to interesting engineering challenges and solutions.

The KVMRT-SBK Line traverses through two geological formations, namely the Kenny Hill Formation and the Kuala Lumpur Limestone Formation. A case history of building/structure protection sited at the Kuala Lumpur Limestone Formation had been discussed in Boon et al. (2015a). This complementary paper discusses three case histories sited at the Kenny Hill Formation, consisting of meta-sedimentary rocks with a thick residual soil layer. The TBMs used in this geological formation are earth pressure balanced (EPB) machine and the variable density machine operating under EPB mode (featured in The European Federation of Foundation Contractors, 2015).

2. BACKGROUND OF TUNNELLING IMPACT

The impact of tunnelling to the surrounding is typically quantified using 'volume loss', which is quantified in greenfield conditions as the area bounded between the original ground level and the settlement trough (Peck, 1969). It is known that several tunnelling operating parameters could affect the volume loss, such as the face support pressure, annulus grouting behind the tailskin, stoppage for intervention, and the stiffness of the tunnel lining (Lee et al., 1992; Loganathan & Poulos, 1998; Thewes & Budach, 2009; Ong & Ng, 2014; Gens et al., 2012). When tunnelling past structures for which the impact is identified to be minimal (by the designers), it is still in the interest of the contractor to assess the risk and adapt its TBM operating parameters accordingly if required. This paper demonstrates an example of this assessment for a structure on raft foundation.

When tunnelling past structures with piles, the piles may experience a loss in mobilised resistance which has to be compensated by more settlements, the magnitude of which will govern whether or not underpinning is required. Furthermore, the new underpinning piles should not experience excessive settlements.

There are a few methods of tunnelling impact analyses on the axial behaviour of piles in the literature. In this paper, the load transfer method (Seed & Reese, 1957; Coyle & Reese, 1966) is adapted further, in which the greenfield settlements are assumed to act as a dragload or negative skin friction onto the pile. To compensate for the loss in mobilised resistance, the required additional settlements are solved iteratively so that the mobilised geotechnical resistance of the pile is again in equilibrium and the imposed pile working load is maintained. This method of analysis is conceptually in the same 'category' of analyses as the boundary element method used in Chen et al. (1999), Chen et al. (2000) and Basile (2014), in which the soil settlements are imposed as the boundary conditions to work out the new pile stresses and displacements. This category of analyses complements (i) other methods based on cavity expansion to calculate the percentage loss in geotechnical capacity (Poulos & Deng, 2004; Marshall, 2012), (ii) methods based on establishing influence zones (Jacobsz et al., 2004; Kaalberg et al., 2006), (iii) methods based on numerical analyses using 2-D finite element analyses requiring rationalisation to 3-D (Ong, 2008) or special elements to model piles (the embedded pile row feature in PLAXIS ver. 12, Sadek & Shahrour (2004)), and (iv) the more rigorous and time-consuming 3-D finite element analyses (Mroueh & Shahrour, 2002; Lee & Ng, 2005; Ong, 2015). The use of springs in the load transfer method and the calculations to work out the required additional settlement to compensate for the loss in mobilised resistance are more intuitive compared to the other methods. The load transfer is easier to apply compared to the boundary element method, and it can be implemented into a MS Excel

spreadsheet through which the equations could be solved using the Solver Tool.

It is known that different elevations of pile toe relative to the tunnel position can lead to different axial pile behaviour (Lee & Chiang, 2007). In this paper, the use of the load transfer method is demonstrated for piles terminating at an elevation above the tunnel crown and piles terminating below the tunnel invert. The following analyses also consider the influence of (i) a potential soft base for bored piles and (ii) pile groups.

Influence zones are then presented in this paper for the different types of pile behaviour. Results from the t-z and Q-z analyses are compared with the influence zones by Jacobsz et al. (2004) based on centrifuge tests, and they are found to have similar trends.

3. CASE HISTORIES

The case histories are discussed in an order following which the risk is increasing. In the first case history, the TBM had to mine past a 15-storey tower founded on a raft foundation. In the second case history, the TBM has to mine past underneath the piles of an existing road bridge. In the third case history, the piles of a Light Rail Transit (LRT) were in the way of the tunnel. These piles had to be removed, and the structure had to be underpinned, with the new piles terminating below the tunnel.

The Kenny Hill Formation, relevant in this paper, consists of meta-sedimentary quartzite and phyllite with a thick residual soil layer consisting of sandy silt and silty sand. References to the soil properties of the Kenny Hill Formation can be found in Wong & Muhinder (1996), Nithiaraj et al. (1996), and Kok (2006). As with most metro projects in the South East Asian region, the parameters adopted for soil strength and stiffness are established from site/laboratory investigation to correlate with the SPT-N value and the type of geological formation. In this KVMRT-SBK Line project, based on literature survey and the extensive data collected from the site investigation programme, a correlation of undrained Young's modulus $E_{50} = 2 \times$ SPT-N was adopted for the Soil Hardening model in PLAXIS (Schanz et al. 1999) with an unloading and reloading stiffness of three times its loading stiffness. The drained loading stiffness is 0.87 times the undrained stiffness. The horizontal to vertical stress ratio, K_0, of 0.8 was used in the project, which is a commonly adopted value for soils. The following strength parameters are adopted as shown in Table 1:

Table 1 Kenny Hill Formation parameters adopted in the KVMRT SBK Line

SPT-N	*Bulk density, γ (kN/m³)*	*Effective cohesion, c' (kPa)*	*Effective friction angle, φ' (°)*	*Young's modulus, E_{50}' (MPa)*
$N \leq 30$	18.5	5	28	0.87 (2N)
$30 < N \leq 100$	19	10	28	0.87 (2N)
$N > 100$	20	15	29	0.87 (2N)
$N > 200$	20	15	38	250
Grade IV rock	20	30	34	250

The soil parameters consistent with the project were adopted in this study, since these analyses resemble the actual engineering considerations that were made prior to tunnelling. That is to say, these case histories reflect in greater emphasis the pre-tunnelling geotechnical considerations in the project than back analyses.

The 0.275 m thick tunnel lining with outer diameter of 6.35 m and inner diameter of 5.8 m was modelled using the in-built function in PLAXIS with the following properties as shown in Table 2:

Table 2 Tunnel lining parameters adopted in analyses

Parameters	*Magnitudes*
EA	7700000 kN/m
EI	48500 kNm²/m
v	0.2

3.1. Tower on raft foundation

The tunnel alignment shortly after the proposed Bukit Bintang Station passes a 15-storey tower building with 4 storeys of underground basement.

3.1.1 Background and description of analyses

The twin tunnels are stacked at this location. The relative distance between the building structure and the twin tunnels is as shown in Figure 1. One of the main reasons of concern for this structure is the potential influence of the tunnelling works on the structure due to location and proximity of the tunnels in relation to the building (see Figure 1).

In order to evaluate the impact of tunnelling works on the structure, 2D finite element (FE) analyses were carried out (see Figure 2).

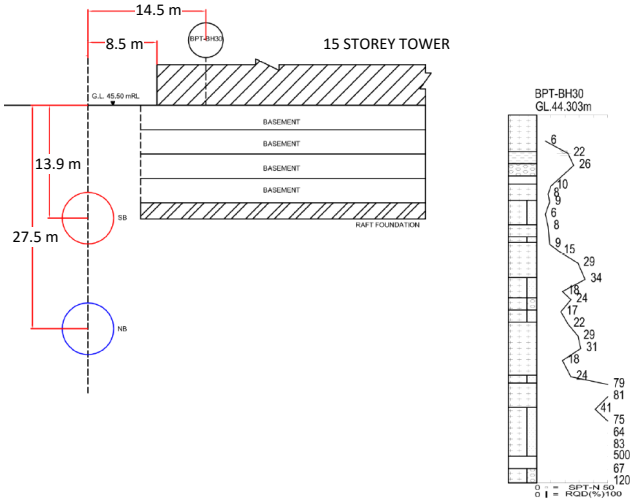

Figure 1 Typical section and profile of SPT with depth (not to scale)

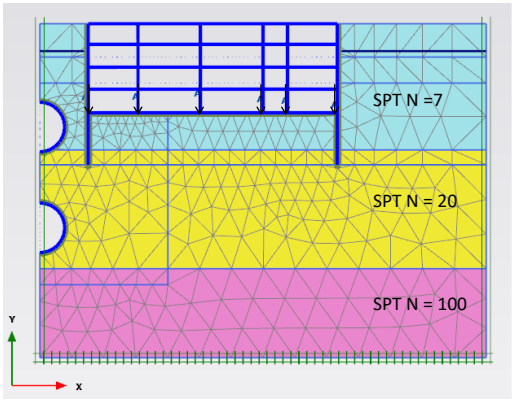

Figure 2 PLAXIS cross-section (building loads are applied as point loads on columns)

Strictly speaking, 3D analysis should be carried out in order to study the TBM face support condition. However, a 2D FE analysis is more economical and the solution is a reasonably conservative approximation to the more complex and laborious 3D analyses. Only the basement of the structure was modelled. The column loads from the 15-storey tower building were assumed to act as loads at the raft. The loads were derived by assuming 15 kPa of surcharge per storey.

The impact was studied based on (i) Method 1: changing the internal tunnel pressure acting on an impervious membrane and also by using an alternative approach of (ii) Method 2: volumetric contraction of the tunnel section. Method 1 is particularly useful in the assessment of face support requirements during TBM mining. The above mentioned techniques are quite commonly adopted for such studies.

The commercial finite element software, PLAXIS version 11, was used. The Soil Hardening model (Schanz et al., 1999) and drained analyses were adopted. At this location, the ground water table is about 3.7 m below existing ground level based on the nearby boreholes. The parameters are as shown in Table 3. Table 4 shows the properties of the raft and column respectively.

Table 3 Soil parameters for finite element analysis (in Figure 2)

SPT N	γ (kN/m^3)	c' (kPa)	φ (°)	E' (MPa)	E_{ur}' (MPa)
7	18.5	5	28	12.2	36.5
20	18.5	5	28	34.8	104.4
100	19	15	29	174	522

Table 4 Raft properties and column properties

Structural element	*EA (kN/m)*	*EI (kNm^2/m)*
1.5 m thick Raft	3.9×10^7	7.3×10^6
0.28 m thick slab	7.3×10^6	4.75×10^4
1.3 × 0.6 m column (11 m spacing)	1.8×10^6	5.5×10^4
0.46 m thick diaphragm wall (0.7 EI was adopted to account for panel jointing)	1.2×10^7	1.47×10^5

3.1.2 Correlating internal pressure with volume loss

Figure 3 is a plot of the internal pressure within the opening (refer to left *y*-axis) and the volume loss (refer to right *y*-axis) against the maximum settlement trough under greenfield conditions. The maximum settlement trough is the settlement at the centerline of the settlement trough at ground surface. In this study, the invert of the tunnel has been fixed so that settlements are mainly derived from the soil settlement above the tunnel. This is carried out for the convenience of correlating the "surface volume loss" against the in-built function of "contraction" in PLAXIS, because the ratio is almost 1:1 when the invert is fixed. A discussion of the fixing of the invert during "contraction" is given in Boon & Ooi (2016).

From Figure 3, the settlement of the trough is roughly proportional to the volumetric contraction of the tunnel section (solid line in Figure 3). It is interesting to note that the settlement of the trough increases in a non-linear manner as the internal pressure is reduced (dashed line in Figure 3). It is expected that as the internal pressure approaches the limiting value, the settlements increase significantly. From Figure 3, the settlement of the trough is about 9 mm for 1% volume loss and this matches the results obtained for an internal pressure of about 290kPa. The internal pressure in the analysis is used to simulate the pressure relief inducing ground loss, which could be affected by the face support pressure, annulus grouting behind the tailskin, stoppage for intervention, and the stiffness of the tunnel lining (Section 2). In Boon (2013) and Boon et al. (2015 b), it is demonstrated that the interface stiffness between the lining and ground is also an important parameter. For reference only, the operating TBM face pressure mining under similar ground conditions is 300 kPa (taking into consideration the cover depth, engineering properties of soil and groundwater level).

Figure 4 is a plot similar to Figure 3 but with the presence of the underground basement (see Figure 2 for PLAXIS cross section). The results show that a higher internal pressure (340 kPa compared to 290 kPa) is required in order to match the settlements obtained using a contraction of 1%. An internal pressure of 290 kPa corresponded to a volumetric contraction of 2.1%, i.e. an increase of 1.1 % compared to the greenfield case obtained previously.

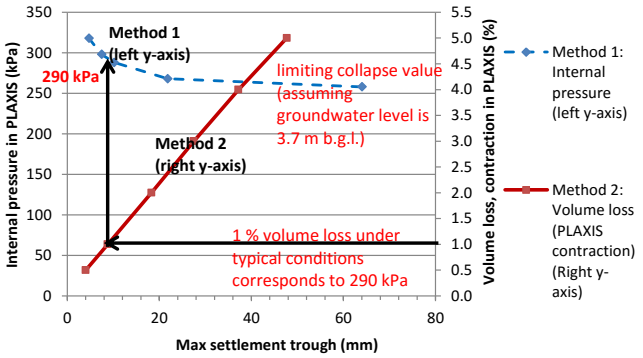

Figure 3 Plot of internal pressure and volumetric contraction against trough settlement for greenfield conditions

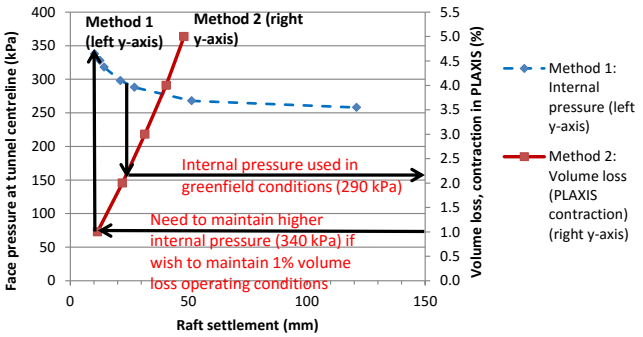

Figure 4 Plot of internal pressure and volumetric contraction against trough settlement with underground basement of tower building

3.1.3 Discussion of prediction and actual performance

Establishing a correlation between internal pressure and volume loss enables the engineer (designer) to verify whether or not it is justifiable to use the same magnitude of volumetric contraction when mining past a structure whose foundation may interact with the tunnel. It is also noteworthy that, if the internal pressure method is adopted without establishing a correlation first as was done in this study, it would be difficult to compare against a benchmark case, i.e. the typical operating performance of the TBM in greenfield conditions.

For the case of tunnelling through this structure, our analyses demonstrates that, with the presence of the building, the analysis requires an additional internal pressure of 50 kPa to maintain the operating condition of less than 1% volume loss for the set of assumptions adopted. This finding is not surprising as some investigators have noted that the magnitudes of settlement are sensitive to the building weight (Burd et al., 2000). Although 3-D analysis would be more appropriate in our study, it was considered conservative to increase the TBM face pressure by approximately 50 kPa based on the results obtained in 2-D analysis. It also would be advantageous to keep the TBM chamber full when traversing this short stretch.

The settlements and distortions from different combinations of volume losses are plotted in Figure 5 and Figure 6 respectively. The impact onto the tower due to different mining sequences of the stacked tunnels was also explored. It is unlikely that the structure considered above would have much damage related issues during tunnel due to the high volume loss before damage occurs. An 'Alarm' is breached only when both thresholds on settlements and distortions are breached. Therefore, for typical operating volume losses, it is unlikely that an Alarm would be triggered (as shown in Figure 6).

The actual face pressure was 340 kPa. The settlement induced by TBM mining was very minimal, approximately an average of 1 mm of settlement was measured from the building settlement markers installed at the 1st basement of the structure. The settlement markers were installed at the 1st basement to allow the transfer of the measurement to the reference survey point on the surface. The results imply that the actual volume loss is minimal and the current soil-structural models/assumptions adopted in the analyses leads to conservative estimates.

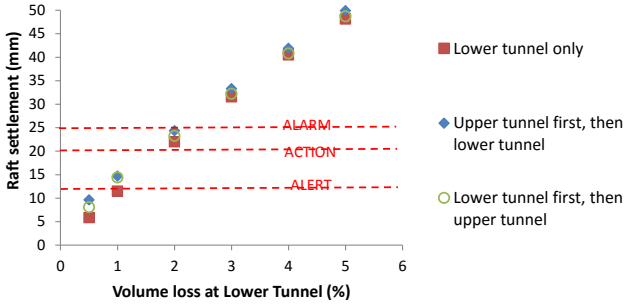

Figure 5 Plot of volumetric contraction against raft settlement

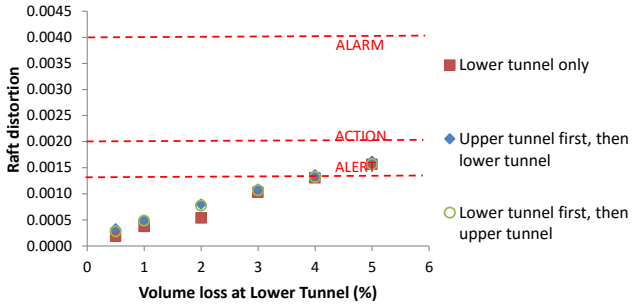

Figure 6 Plot of raft distortion against volume loss

3.2 Flyover Bridge

The tunnel alignment passes through an existing bridge (see Figure 7), which has heavy traffic flow in Kuala Lumpur.

Figure 7 Photo of Flyover

The bridge is believed to be constructed in the 1960s, and was widened by approximately 9.4 m in 1999 to accommodate a new ramp. The widening was supported on a different beam-pier system, which is M-shaped (see Figure 7). The bridge consists of 4 spans in total, and is supported by 30 reinforced concrete piers. The twin tunnels in this project had to be constructed underneath this structure, as shown in Figure 8.

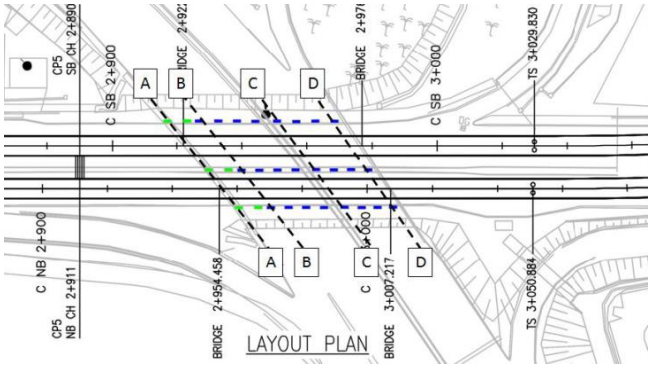

Figure 8 Layout plan of Flyover

3.2.1 Site investigation

The as-built drawings for the original bridge were not available, and only the 6 piers constructed during the widening had as-built drawings. The as-built drawings for the widening part were available, showing that this part of the bridge was founded on 1.2 m diameter bored piles. During the first stage of soil investigation, boreholes were carried out, and hard material was encountered 9 – 13.5 m bgl. Parallel seismic surveys were carried out from the same boreholes to confirm and detect the actual pile lengths.

During the second stage of investigation, five trial pits were carried out to expose the pile type underneath the pile cap. A combination of H-piles (300 mm), bored piles (900 mm) and concrete block were found. More parallel seismic investigation was carried out to determine the actual pile length. A more detailed discussion of the investigation works can be found in Mak et al. (2015).

The permissible settlements and differential settlements which were adopted in the project are 12 mm and 1:1000 respectively.

3.2.2 The use of t-z and Q-z method for predicting settlements

The layout plan has been shown previously in Figure 8. One of the cross sections, A-A (widening part of the bridge), which was referenced for analysis in this paper, is shown in Figure 9.

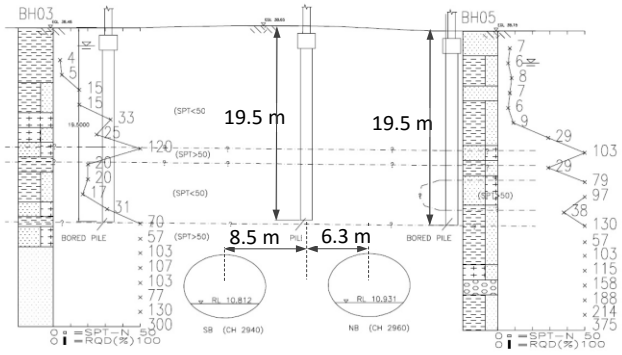

Figure 9 Cross-section A-A in Figure 8 (not to scale)

The load-transfer method (Seed & Reese, 1957; Coyle & Reese, 1966) is used. The t-z and Q-z curves were obtained from axisymmetric analysis of a single pile for different working loads (Figure 10) using PLAXIS, and the soil parameters adopted are shown in Table 5. An interface factor R_{inter} = 0.67 was adopted, since

the structure-soil friction angle is typically adopted as 2/3 the soil friction angle in design (Atkinson, 2007). The results are shown in Figure 11. These values are provided by PLAXIS when clicking at the interface. For multi-layer soils, deriving the t-z and Q-z curves from finite element analysis is easier compared to analytical solutions, e.g. Randolph & Wroth (1978) and Kraft et al. (1981). In practice, it is noted that the end bearing stiffness obtained from idealized soil profiles is high, as there could be a possibility of a lower end bearing stiffness due to the presence of debris at the base of the bored piles (Poulos, 2005). Analyses were carried out to explore the influence of the presence of a soft layer (E'_{50} = 8700 kPa, c = 1 kPa and φ = 28°), with thickness between 10 – 20 cm at the base. The end bearing stiffness with the softer toe is shown in Figure 11(b). The results indicate that, for this specific case, the end bearing stiffness is more than seven times lower when a soft base is present. The thickness of the soft material increasing from 10 cm to 30 cm did not appear to have a huge impact, and the end bearing stiffness is still stiffer than the shaft stiffness.

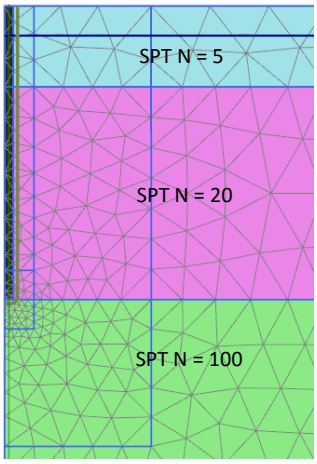

Figure 10 Axisymmetric analysis of a single pile

Table 5 Soil parameters for finite element analysis (see Figure 2)

SPT N	γ (kN/m³)	c' (kPa)	ϕ (°)	E' (MPa)	E_{ur}' (MPa)
5	18.5	5	28	8.7	26.1
20	18.5	5	28	34.8	104.4
100	20	15	29	174.0	522

Greenfield settlements are obtained from PLAXIS (Figure 12) and the settlements experienced by the different piles are shown in Figure 13. It is noted that measurements of greenfield settlements using extensometers were unavailable at this site, but at other locations in the projects the extensometer readings generally showed consistent trends with the sub-surface Gaussian settlement profile given by Mair et al. (1993). A comparison of the predictions obtained from PLAXIS and the equations in Mair et al. (1993) are compared later in Section 4.

The calculated settlements are given as input to the load-transfer method, as illustrated in Figure 14. Note that the limiting shaft resistance is taken as 2×SPT-N. In the analysis here, an iterative procedure was used to seek the settlement required to match the cumulative resistance from the toe with the imposed pile working load at the top of the pile. The calculations are explained in Appendix A.

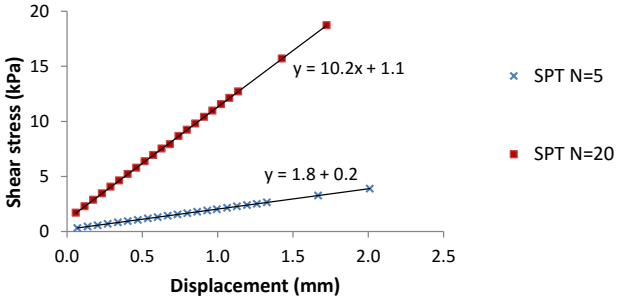

(a)

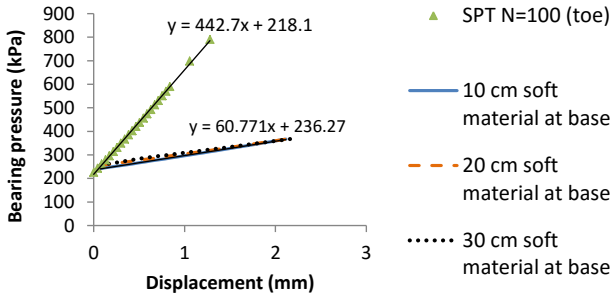

(b)

Figure 11 Resistance obtained from the axisymmetric analysis for (a) shaft and (b) end bearing. The y-axis intercepts are ignored when assigning the stiffness values into the t-z and Q-z analyses.

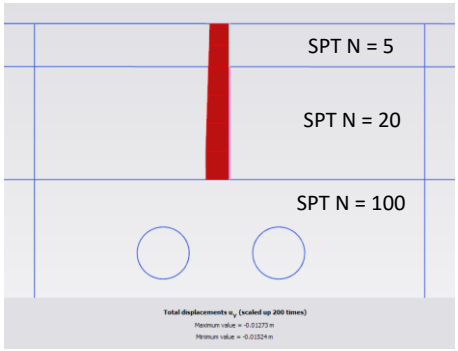

Figure 12 PLAXIS analysis of twin tunnels (representative of the few cross-sections in Figure 8) to derive greenfield settlements

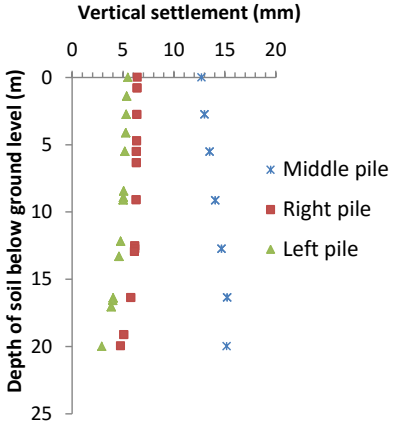

Figure 13 Settlements derived from PLAXIS analysis in Figure 12

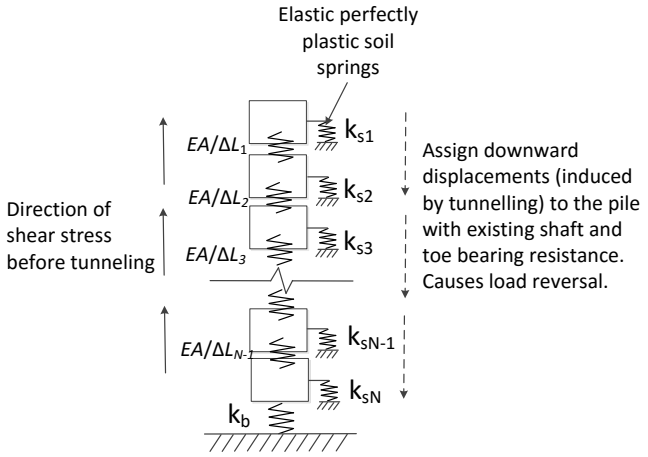

Figure 14 Load Transfer Method (after Coyle & Reese, 1966).

The result of the analysis from the load transfer method in Figure 15(a) and (b) shows, for the piles of the middle and right piers respectively (Figure 9), the new load distribution with depth after equilibrium to compensate the out-of-balance conditions due to a loss in mobilised resistance resulting from tunnelling.

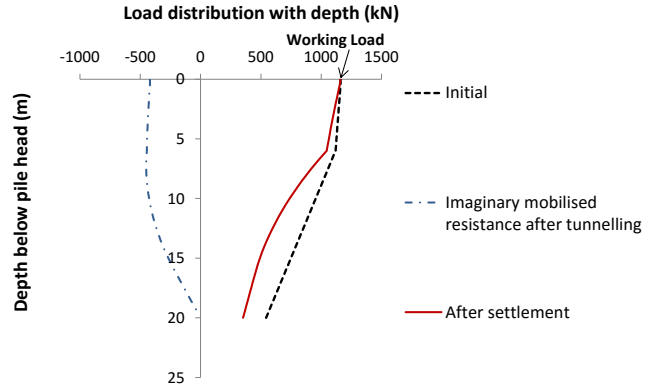

(a)

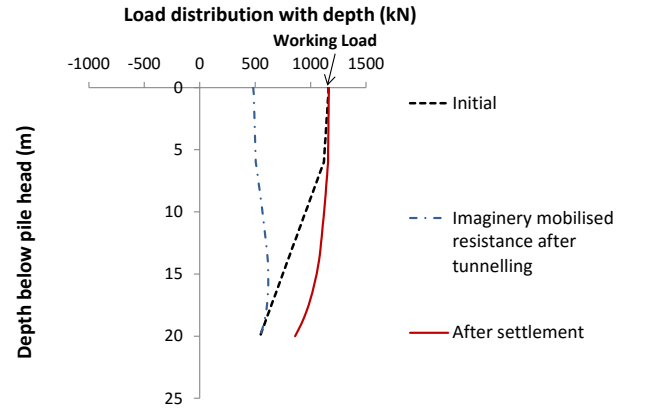

(b)

Figure 15 Analysis for the pile: (a) in the middle (soil settlement increasing with depth), and (b) on the right (soil settlement decreasing with depth). Load transfer with depth.

The loss in mobilised resistance as plotted in Figure 15 are annotated as 'imaginary' because the actual loads in the piles occur gradually in the transient case, and the piles do not experience such large magnitudes of negative skin friction at any given time. The assumption of aggregating the total negative skin friction occurring in one instance during tunnelling is necessary to facilitate the solution process for the analysis.

The shaft resistance (kPa) and bearing pressure (kPa) are shown in Figure 16(a) and (b) respectively for the middle and right pile. There is loss of end bearing pressure for the middle pile, and increase of end bearing pressure in the right pile. The reason is that the soil settlements increases with depth for the middle pile and the toe experienced the greatest settlement. On the other hand, the soil settlements decreases with depth for the left and right piles (see Figure 13). These observations explain the trend in the mobilised loads which is discussed in the next paragraph.

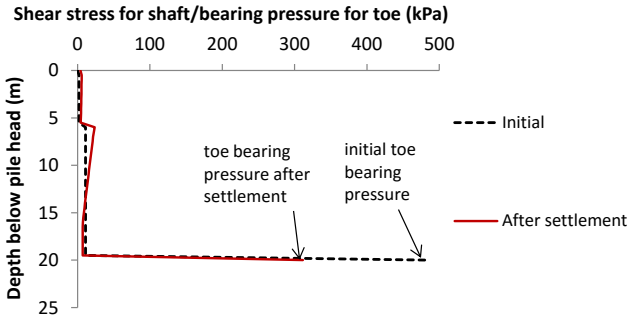

(a)

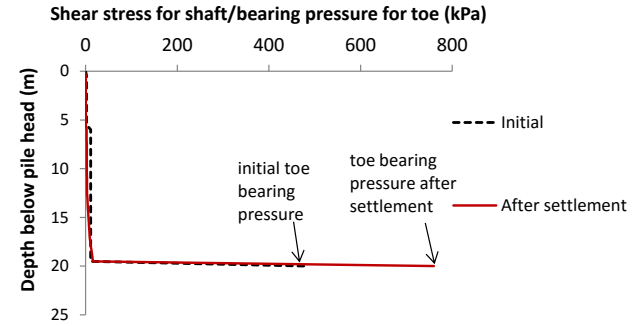

(b)

Figure 16 Bearing pressure or shear stress along the pile (a) in the middle and (b) at the right

The results revealed two types of pile behaviour. In the analyses here, a gap is assumed to form underneath the pile toe for the middle pile, since the settlement at the toe is greatest along the pile. In the first case, the pile could not breach the gap at the toe. The shaft resistance mobilised by further settlements was able to compensate most of the loss in mobilised resistance, before the end bearing resistance begin to mobilise (solid red line in Figure 15(a) and Figure 16(a)). Similar results were obtained in centrifuge tests by Lee & Chiang (2007) (Figure 15(b) in their paper), for the case when the pile toe is at an elevation higher than the tunnel. In the second case (right pile), there is no gap underneath the pile toe, since the soil settlements at the toe relative to the pile body is smallest. In this case, the pile was able to mobilise higher end bearing resistance, and did not have the chance to mobilise as much shaft resistance compared to the middle pile (solid red line in Figure 15(b) and Figure 16(b)). Similar findings were found in centrifuge tests (Figure 15(a) in Lee & Chiang (2007)).

It is noted that the mobilised end bearing resistance in Figure 15 are noticeably high relative to the total mobilised loads, based on the local experience of load tests on bored piles in the Kenny Hill Formation; a literature survey is given in Ooi & Khoo (2016). The numerical results here were obtained because the pile is founded on SPT-N 100 soil, by comparison to SPT-N 20 soil in the shaft.

The results with a soft material at the base of the pile are shown in Figure 17. Compared to the case without the soft base, the initial

mobilised resistance is different but the same trend was found. With a soft base, the magnitudes of the rise or drop in end bearing pressures due to tunnelling are smaller.

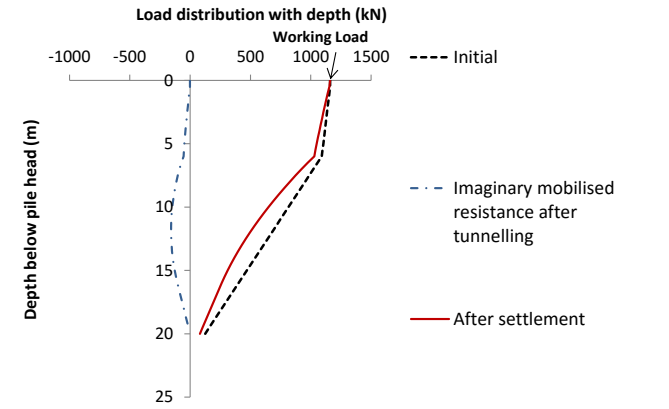

(a)

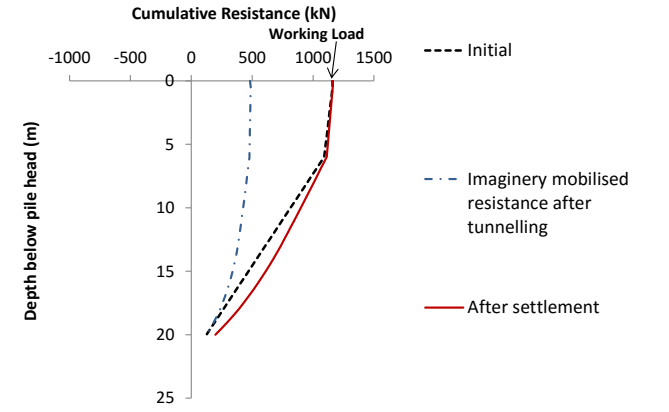

(b)

Figure 17 Analysis for the pile with a soft base at the pile toe: (a) in the middle, and (b) on the right: load transfer with depth

A comparison between the predicted and measured settlements for the two rows of piers (new bridge extension) is shown in Table 6. The calculated settlement magnitudes (without the soft base) are 14.9 and 5.4 mm respectively for the middle and right pile. The actual measured settlements are approximately on average 8.5 and 5.8 mm respectively (see Table 6). The reported settlements are the settlements induced by tunnelling. An interesting finding is that, when compared to the case without the soft base, the settlement with the soft base is marginally smaller for the middle pile (soil settlement increasing with depth), but marginally higher for the right pile (soil settlement decreasing with depth). The reason is that the mobilised end bearing pressure under the original working conditions for the middle pile without the soft base is greater, and the pile experienced a greater reduction in mobilised resistance (end bearing) due to the ground movement induced by tunnelling.

Table 6 Predicted vs Measured Settlements

	Predicted Settlements (mm)	**Measured Settlements Row 1 (mm)**	**Measured Settlements Row 2 (mm)**
Middle pile	14.9 (14.6)*	8.6	8.5
Right pile	5.4 (5.9)*	6.6	5.0

* indicates assumption of a softer pile base

When compared to field measurements, the results suggest that the t-z and Q-z method appears to give conservative estimates for the middle pile. These could be due to several reasons, such as the ignoring of the bridge stiffness, possible smaller magnitudes of actual volume loss and localized variation in soil profile. Note that 1 % volume loss was assumed in the analyses and could be a conservative estimate. This magnitude of volume loss is a typical value that was adopted for design in the project. Smaller magnitudes of volume loss had been recorded from ground settlement markers in the vicinity of this location.

3.3 Light Rail Transit (LRT)

From site investigation, seven of the piles of the Light Rail Transit (LRT) (see Figure 18) were in the way of the tunnel alignment. The LRT has to remain operational to the public throughout the tunnelling works. The overall protection measure for this structure is discussed here. The piles within the tunnel horizon (red dots in Figure 19) had to be removed and underpinning had to be carried out (the new columns are highlighted as blue squares in Figure 19). Cross sections A-A and B-B are shown in Figure 20(a) and (b).

Figure 18 LRT Station

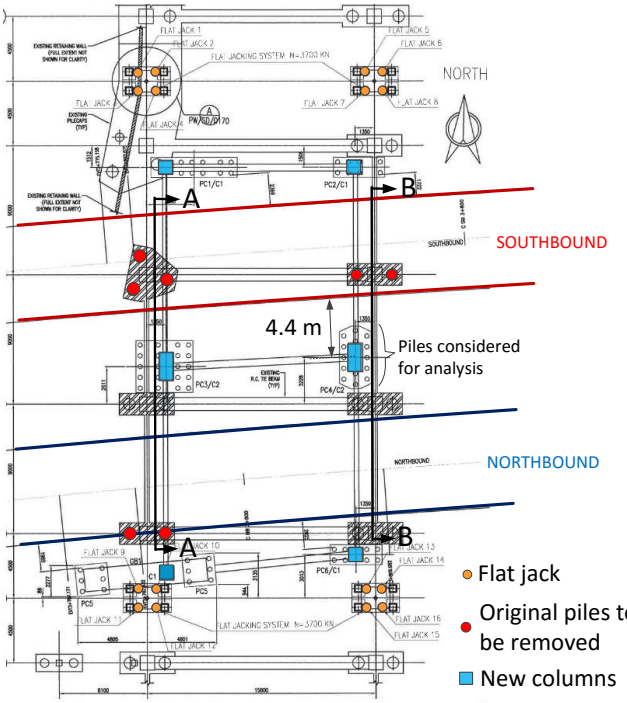

Figure 19 Layout plan of affected piles at LRT station

3.3.1 Underpinning works

Columns whose foundation piles are affected had to be disconnected and the LRT station had to be underpinned with new columns and piles (see Figure 21). The new piles, consisting of 300 mm diameter micropiles, were installed away from the tunnel horizon and were designed to socket 7.5 m into rock or Grade IV material.

Transfer beams are installed underneath the LRT stations to connect to the new columns. The new columns are jacked so that the

loads from the station are transferred to the new underpinning piles, and the old columns are disconnected (see Figure 21).

Because the soffit of the new pile caps are 4 m below ground, it was necessary to have a temporary works design for this construction. A soldier pile timber lagging wall with a layer of strut was used to retain the soil for the construction of the pile cap.

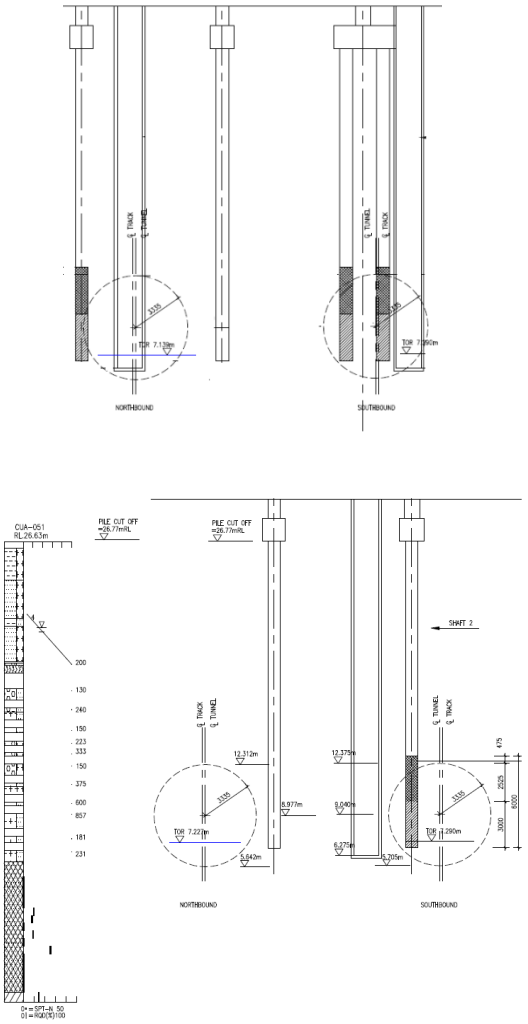

(a)

(b)

Figure 20 Cross-sections (a) A-A and (b) B-B in Figure 19. Pile bodies to be removed are shaded

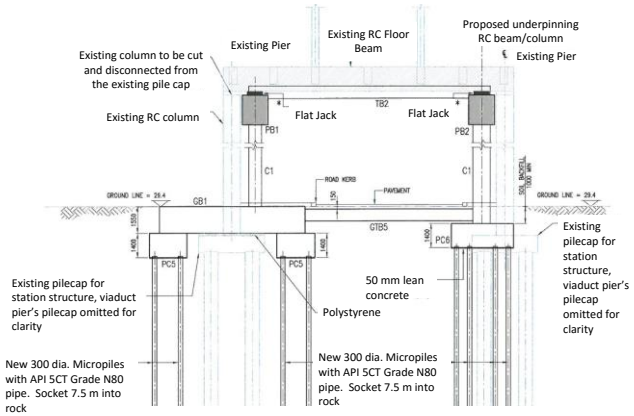

Figure 21 Transfer beam and new columns and piles

3.3.2 Vertical shafts and mined adits for pile removal

Due to space constraints, the piles had to be removed through the construction of vertical shafts and mined adits. The diameters of the vertical shafts are 2.1 m and the shape of the mined adit is horse-shoe shaped. A discussion of the construction of vertical shafts and mined adits can be found in Khoo et al. (2015).

For piles which exist in 3-pile groups, the diameter of a single adit would be too large. These piles were removed by mining an adit horizontally away from the vertical shaft to remove two piles first, after which they are backfilled (see Figure 22). After backfilling the adit, another adit from the same vertical shaft is mined to remove the third pile.

Because of the length of the pile which had to be removed (approximately close to the vertical height of the tunnel), three rows of adits were proposed initially. The lowest row adit is mined first, and, after removing the piles in its horizon, the adit is backfilled. Then, the second row adit is mined immediately above the first row adit which had been backfilled. Similarly, after the piles are removed, the adit is backfilled. Then, the process is repeated for the third row. To speed construction progress, the three rows of adits were reduced to two rows. This is achieved by creating a localised excavation which is deeper at locations where the piles exist and had to be removed. This is discussed in more detail by Khoo et al. (2015). The localised deeper excavation is backfilled immediately. The construction sequence is shown in Figure 23.

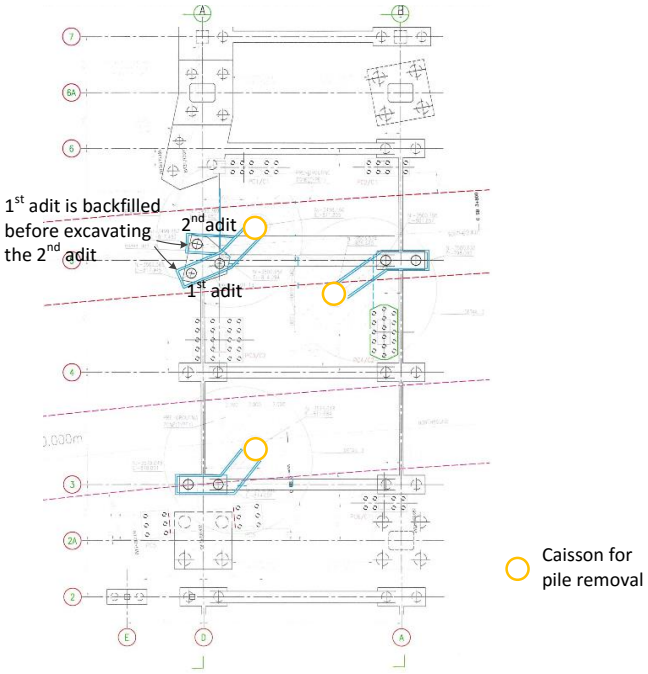

Figure 22 Layout plan for caisson and adit

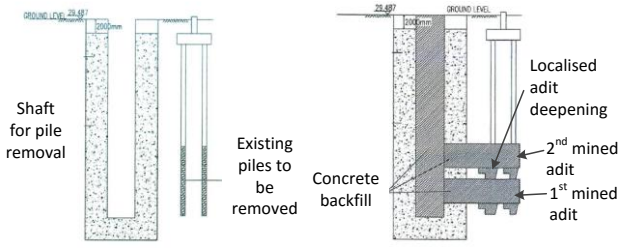

Figure 23 Construction of mined adit for pile removal

3.3.3 Installation of flat jacks

Piles whose geotechnical capacities are affected are also provided with flat jacks or hydraulic jacks underneath the viaducts at the columns so that any potential settlements outside of the permissible tolerance could be corrected in a timely manner (see Figure 24). Note that the maximum permissible settlement and differential settlement are 15 mm and 1:2000 respectively. For every pier which requires a jacking system, a number of four flat jacks are installed (see Figure 24).

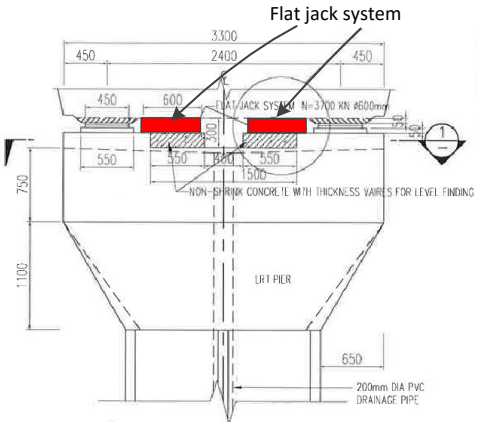

Figure 24 Installation of flat jacks underneath viaducts: cross-section

3.3.4 Instrumentation and Monitoring

The settlement of the structure had to be monitored so that feedback could be provided to the operations teams supervising the TBM mining and jacking the viaducts. The maximum permissible settlement and differential settlement are 15 mm and 1:2000 respectively. Building settlement markers, optical prisms, tiltmeters and electrolevel beam sensors were installed. An hourly monitoring was implemented during adit excavation and pile cutting as well as when the TBM was mining underneath this structure (see Figure 25).

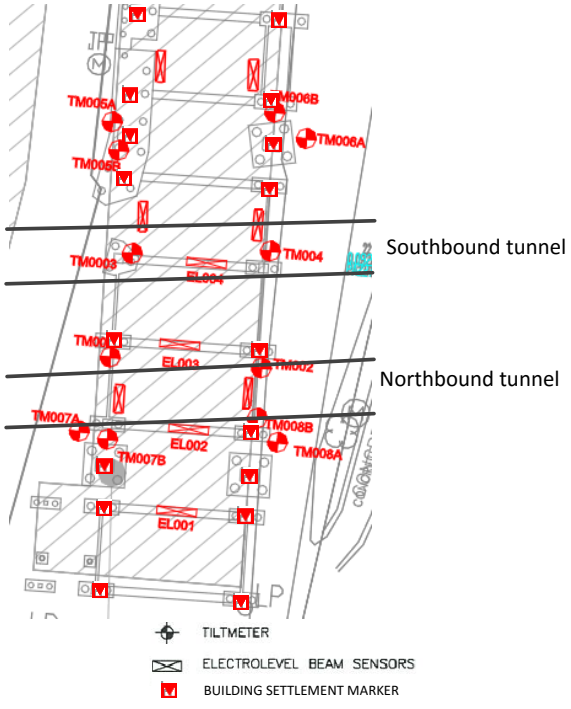

Figure 25 Monitoring instrumentation for LRT

The electrolevel beam sensors were connected to an automated logging system, so that real-time monitoring could be carried out. The fine precision of the instrument, as possessed by the EL beam, was important because the trigger values for Alert, Action and Alarm was 1:4000, 1:2500 and 1:2000 respectively.

3.3.5 Load transfer predictions

A load transfer analysis was carried out for the 300 mm underpinning micropiles. The pile has a working load of 1200 kN and is socketed 7.5 m into Grade IV rock. The analyses were calculated using PLAXIS and the soil properties are shown in Table 7.

Table 7 Soil parameters for finite element analysis (see Figure 26)

SPT N	γ (kN/m^3)	c' (kPa)	ϕ (°)	E' (MPa)	E_{ur}' (MPa)
5	18.5	5	28	8.7	26.1
100	20	15	29	174.0	522
G-IV rock	20	30	34	250	750

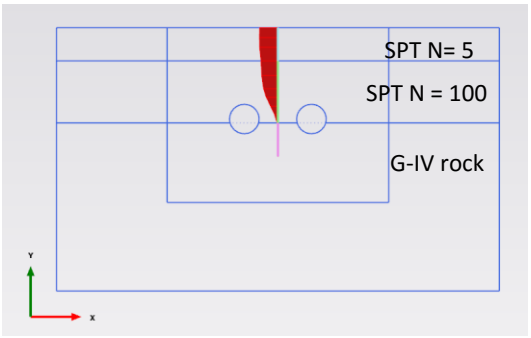

(a)

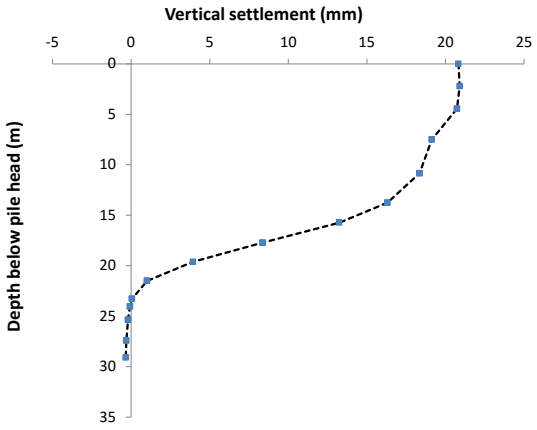

(b)

Figure 26 Greenfield settlements extracted from PLAXIS

The greenfield settlements are shown in Figure 26. The soil springs were calculated in a similar manner to the previous case study using PLAXIS, as shown in Figure 27 (a) and (b). Figure 28 shows the results and the trend is very similar to the results of the previous case history, for the case where the greenfield settlements decrease with depth. The predicted settlement is 0.6 mm. The calculated magnitude of settlement is that for a single pile. The magnitude of pile group settlement is expected to be higher and is a function of L/d (pile slenderness), K_{rel} (compressibility of the pile relative to the soil), s/d (spacing-to-diameter ratio), the pile group size, and the boundary conditions at the pile toe (Poulos & Mettes, 1971). The maximum measured settlement was approximately 4 mm and the maximum recorded distortion from the EL beam was 0.01 mm/m.

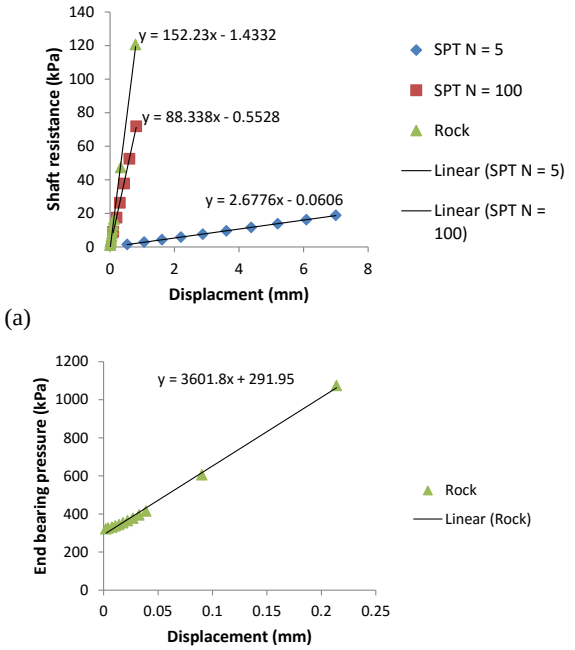

Figure 27 Resistance at different soil layers from PLAXIS for (a) shaft and (b) end bearing, tested within its elastic limit. The y-axis intercepts are ignored when assigning the stiffness values into the t-z and Q-z analyses

4. INFLUENCE ZONES

Based on the findings from the case histories on pile foundations, it was found that there are two general trends for pile axial behaviour induced by tunnelling. The concepts discussed later are similar to the findings of centrifuge tests presented in Jacobsz et al. (2004). Different zones are derived from greenfield settlements obtained in PLAXIS for the second case history (flyover bridge), and is plotted in Figure 29 as dots and crosses. The physical significance of the zones is discussed further based on the results from the *t-z* analysis in this paper (see Figure 29). If the pile toe is within the first zone (Zone A), the pile head settlement is greater than the greenfield ground surface settlement. There is loss of end bearing pressure and consequential increase in mobilised shaft resistance. If the pile toe is within the second zone (Zone C), the pile head settlement is less than the greenfield ground surface settlement, and there is a consequential increase in mobilised end bearing pressure. From the t-z analyses earlier on, this is largely affected by the settlement trends, i.e. Zone A is the region where the soil settlements are increasing, and Zone C is where the soil settlements begin to decrease.

For comparison, these zones were also derived using the Gaussian settlement profile and sub-surface Gaussian settlement profile of Mair et al. (1993). By generating the settlement profiles along the horizontal direction at multiple depths, and later taking the vertical profiles, the points at which settlements begin to decrease are plotted. The slope of the line joining the points was found to be insensitive to the volume loss and cover depth, as shown in Figure 30.

Incidentally, it was found that these points match the curve joining the points of inflection used in the Gaussian functions. From the ground surface till the point of inflection, the settlement shows an increasing trend. Below the point of inflection, it begins to decrease. This is verified by plotting in the function expressing the point of inflection as a function of depth from Eq. (10) in Appendix B.

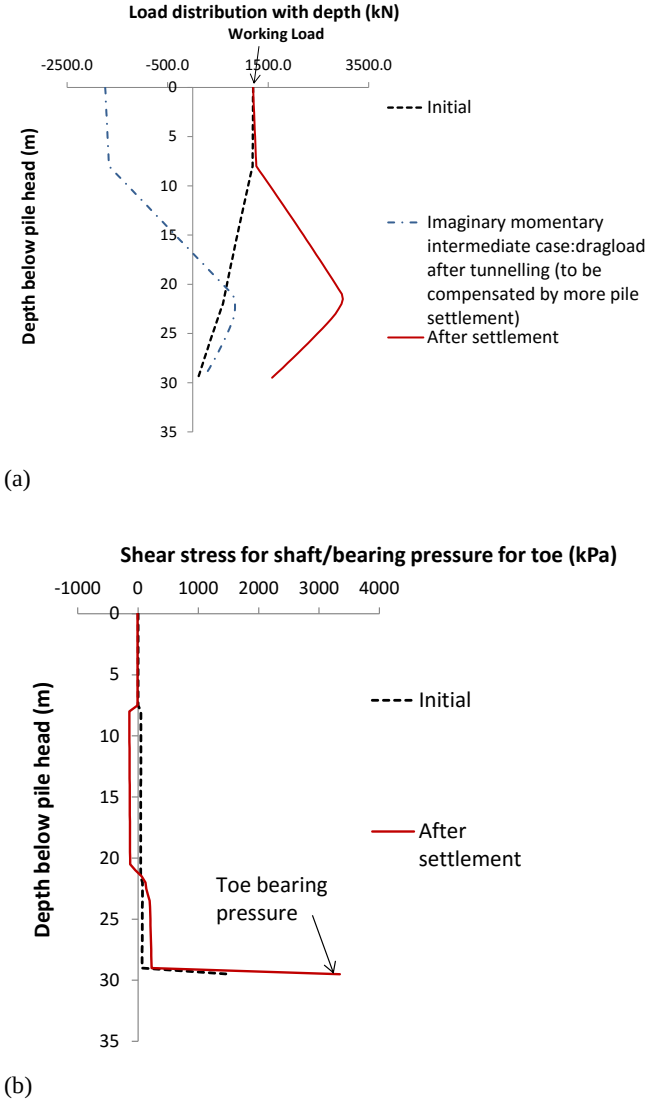

Figure 28 Loads in pile after tunnelling predicted from load transfer analysis for: (a) cumulative mobilised resistance and (b) shear stress/end bearing pressure

The point of inflection has been known to be the point of maximum slope and point of maximum horizontal movement along the horizontal direction (New & O'Reily, 1991). The finding of this paper shows that it has another physical significance along the vertical profile, as mentioned in the paragraph above.

For practical purposes, the settlement magnitudes are equally important compared to the trend of pile behaviour, i.e. whether it falls in Zone A or Zone C. For increasing cover depths, the magnitude of surface settlement decreases. As shown in Figure 30, the settlement magnitude at the ground surface at the line of inflection is 13 mm for a tunnel with cover depth/tunnel diameter (C/D) ratio = 2 (large orange dot in Figure 30). This settlement magnitude (13 mm) occurs at a deeper depth for deeper tunnels. Therefore, the evaluation of impact should be truncated in a vertical manner based on the horizontal distance between the pile and the tunnel (see Figure 31). It appears that this distance is more or less constant for the different cover depths adopted in the investigation, i.e. one diameter from the tunnel centre. Note that 1% volume loss was used in the analyses.

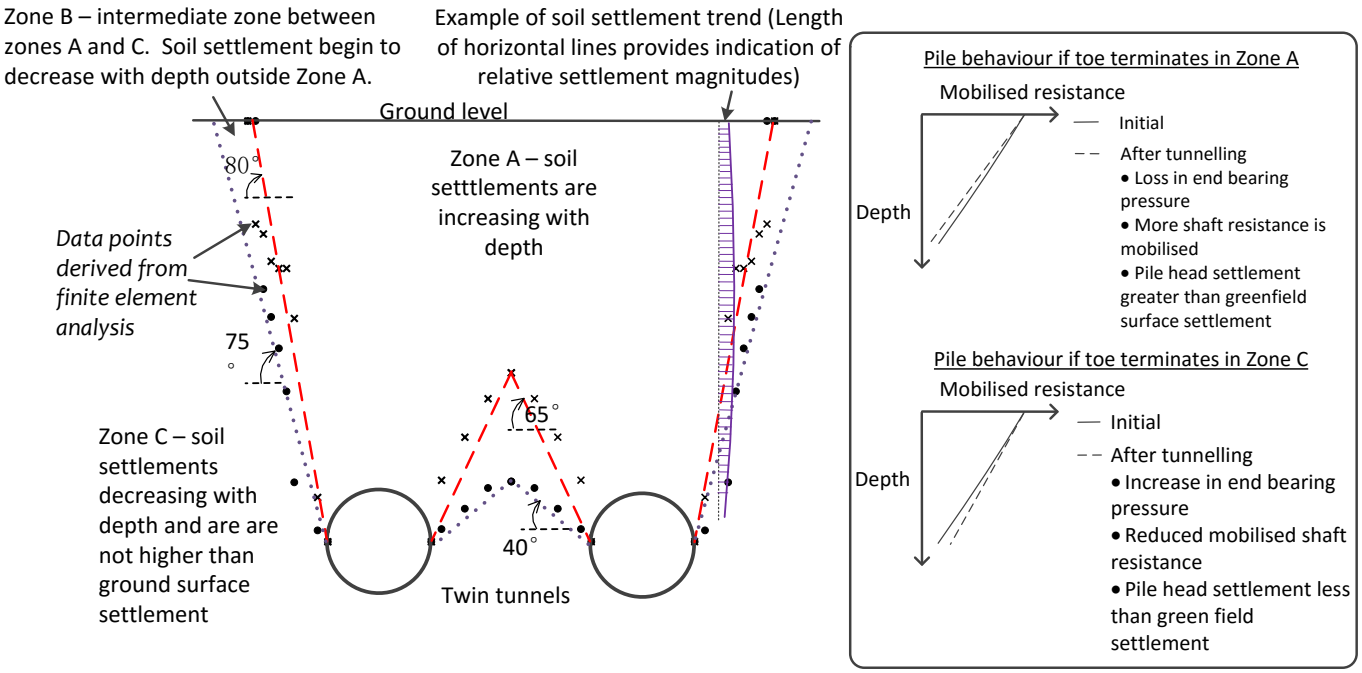

Figure 29 Influence zones established from greenfield settlement trends derived from PLAXIS (black dots and crosses) based on case history two (flyover bridge), and schematic of pile behaviour for the two zones. Compare with Figure 30 (derived from different method). Prediction is mainly for cast-in-place piles.

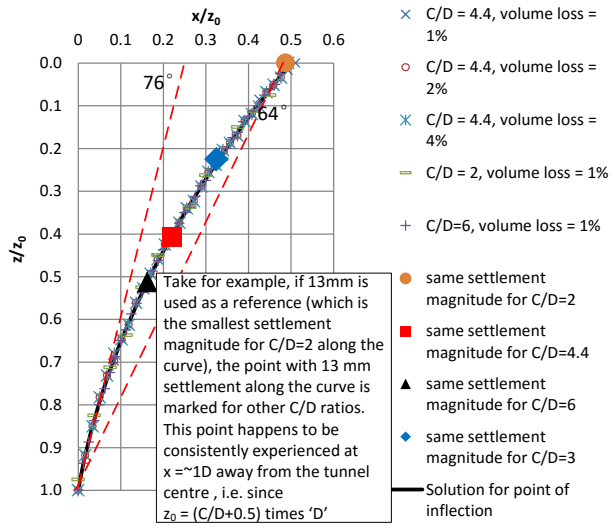

Figure 30 Boundary line denoting maximum settlement in the vertical profile. *C/D* = cover to tunnel diameter ratio, z_0 = depth of ground surface to tunnel centre, z = depth, x = horizontal distance: The 'same settlement magnitude' is for 1% volume loss.

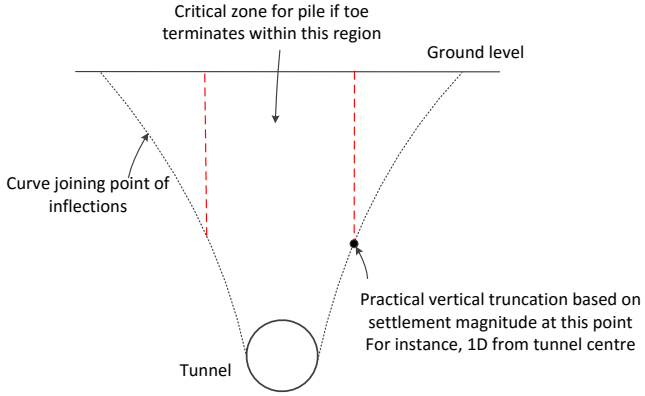

Figure 31 Schematic of practical influence zones with recommended vertical truncation

5. CONCLUSION

Three case histories of tunnelling past critical structures with different risk levels and protection measures are discussed. The engineering considerations and the insights obtained from the analyses are also discussed. These engineering analyses are helpful to assess the level of risk mitigation and protection measures that are required in an underground metro project, as demonstrated through these case histories.

In the first case history, the TBM had to mine past an underground basement. In terms of analyses, this paper answers the question: "Would the presence of this structure affect TBM mining insomuch as the volume loss increases?". A series of analyses had been carried out using two methods of analyses in PLAXIS 2D, namely the internal pressure method (Method 1) and the contraction method (Method 2). Without comparing the two approaches, it is difficult to understand the effect of the building on the induced settlement compared to typical operating conditions in greenfield conditions. The typical operating TBM face pressure under similar ground conditions (soil cover, SPT values, water standpipe level) is 300 kPa. Under greenfield conditions, to match the settlement trough obtained in PLAXIS using a contraction of 1% (Method 2), an internal pressure of 290 kPa is required based on Method 1. The same internal pressure of 290 kPa with the presence of the underground basement corresponded to a contraction of 2.1% (Method 2) to match the settlement magnitudes. To maintain the same 1% volume loss conditions, an internal pressure of 340 kPa was required. Our results indicate that the TBM needs to reduce potential drops in soil stresses due to mining, either by increasing the face pressure or imposing more stringent quality control on the secondary grouting behind the TBM tailskin.

In the second case history of this paper, the pile toes of the flyover bridge are at an elevation above the tunnel. The additional settlements required by the piles to achieve equilibrium after tunnelling is calculated using the load-transfer method (Seed & Reese, 1957; Coyle & Reese, 1966) by providing as input the greenfield settlements induced by tunnelling which would create load reversal to the shaft resistance and loss of bearing pressure at the toe. Note that this method is complementary to the method proposed in Poulos & Deng (2004), which considers the loss in geotechnical capacity due to "radial stresses", but does not consider further pile displacements as a result of this loss. Our method demonstrated in this paper has closer resemblance to the method of Chen et al. (1999) which considers consequential settlements, i.e. the pile may deform further to mobilise higher shaft or base resistance, i.e. compensating for the loss of mobilised resistance in the pile due to tunnelling. The predicted magnitudes of settlement are comparable with measurements and potential causes of discrepancies were discussed. Therefore, this proposed method will be of use in the industry, especially as an alternative to the time consuming 3-D finite element modelling or other equivalent beam methods whose theoretical background is not as straightforward as t-z and Q-z analyses.

In the third case history, the piles of a LRT station were in the way of the TBM. The mitigation measures and design considerations are detailed such as the construction of vertical shafts and mined adits for pile removal, the underpinning of the structure with new transfer beams, columns and piles. The excavation for the construction of new pile caps was achieved using soldier pile timber lagging. The LRT structure was monitored with various instruments, such as building settlement markers, electrolevel beam, tiltmeters and optical prisms. The LRT experienced very minimal settlements and differential settlements.

Approximate methods to account for the effects of soft toes in bored piles and pile groups are also discussed. From the analysis with the soft toe, we found that the shaft and end bearing (relative) stiffnesses were capable of affecting the mobilised resistance along the pile. In addition, the magnitudes of settlement for a pile group will be underestimated by analyses based on a single pile, and corrections have to be made.

Influence zones are proposed for the different types of behaviour. The results obtained from this t-z and Q-z analyses show similar trends to the previous findings in Jacobsz et al. (2004) from centrifuge tests. A more thorough explanation is obtained as to why at some regions the pile settles more than the surface and otherwise at other regions. This behaviour depends on where the pile toe terminates, i.e. whether or not the soil settlement along the pile is always increasing with depth.

The results obtained in the load transfer analyses for both case histories show that the soil settlement trends along the pile would serve as a more robust indicator of the axial loads experienced in the pile after tunnelling. For the case where the soil settlement increases with depth along the entire pile (Zone A in Figure 29), the pile compensates the loss of mobilised resistance mainly through its shaft resistance. For the case where the pile terminates in areas where the soil settlement decreases with depth (Zone C), the pile compensates the loss of mobilised resistance mainly through end bearing. This finding explains the pile axial behaviour observed in Lee & Chiang (2007) obtained from centrifuge tests. The agreement between field measurements in this paper and similar trends observed in centrifuge tests by other investigators (Lee & Chiang, 2007; Jacobsz et al., 2004) substantiates this method of analyses (Appendix A).

It is also shown here that the line joining the points of inflection for several layers of sub-surface Gaussian settlement profile in Peck (1969) can be used to define the boundary between settlement trends of (i) increasing with depth and (ii) decreasing with depth, i.e. Zone A and Zone C respectively.

6. ACKNOWLEDGEMENT

The analyses and discussion undertaken here do not indicate a preference among the different types of analyses for tunnel-foundation interaction by the authors and the institutions to which the authors are affiliated.

7. APPENDICES

7.1 APPENDIX A – Calculation procedures for t-z and Q-z analyses

The calculation procedures to obtain the pile settlements used in the paper are explained. From Coyle & Reese (1996) (also in Poulos & Davis (1981)), assuming that there is a linear variation of load in a segment with length, ΔL, the elastic deformation of the midheight of the segment, u_e, is calculated as:

$$u_e = \left(\frac{Q_m + P_{prev}}{2}\right)\left(\frac{\Delta L}{2AE}\right) \quad (1)$$

where

$$Q_m = \frac{Q_{top} + P_{prev}}{2} \quad (2)$$

$$Q_{top} = \pi D \Delta L k_s u_s + P_{prev} \quad (3)$$

$$P_{toe} = k_b u_{toe} \quad (4)$$

The shaft and toe stiffness is denoted as k_s and k_b respectively, and the shaft and toe displacements are denoted as u_s and u_b. The cross-sectional area of the pile is denoted as A, the Young's modulus as E. The cumulative resistance at the bottom of the segment is P_{prev} and is equal to P_{toe} for the bottommost segment.

The shear displacement experienced by the pile segment is the sum of the elastic shortening and the toe displacement:

$$u_s = u_e + u_{toe} \quad (5)$$

To work out the mobilised resistance along the pile, it is necessary to calculate the shear displacement, u_s, by substituting (1)-(3) into (5). This results in the following:

$$u_s = \frac{u_{toe} + \frac{3P_{prev}\Delta L}{8EA}}{1 - \frac{\pi D \Delta L k_s}{8EA}} \quad (6)$$

from which one can use to derive the P_{prev} at every element, once the parameter u_{toe} is assigned. The variable u_{toe} is sought iteratively as explained in the following paragraphs. When the shaft resistance, $k_s u_s$, at a segment exceeds its limiting resistance, the value is capped (based on SPT N correlations e.g. in Chang & Broms (1991) for residual soils). The limiting shaft resistance, $f_s = 2\ N$, is assumed in this paper.

At the topmost element, Q_{top} must be the same as the pile working load. This objective function is satisfied by changing u_{toe} iteratively. The solution can be obtained easily from the Solver tool in MS Excel.

This iteration procedure is carried out to establish the mobilised shaft resistance at the beginning of the analysis. After tunnelling, the greenfield settlements are separated into en-block and relative movement between the pile head and pile toe (see Figure 32). The relative movement causing a negative skin friction/downdrag is added onto the original mobilised resistance, P_{prev}. The iteration procedure is carried out again to calculate the settlements required so that the mobilised resistance at the pile head is again equal to the working load. The axial compression of the pile is implicitly re-calculated using Eq. (6). The total settlement is the sum of the en-block movement and the additional settlements required to achieve equilibrium due to the negative skin friction/dragload.

An elastic-perfectly plastic soil spring is used here in this paper to model the soil spring at the shaft. Note that it is possible to obtain a solution even with non-linear spring models using the Solver tool in MS Excel insomuch as the behaviour can be expressed in closed-form.

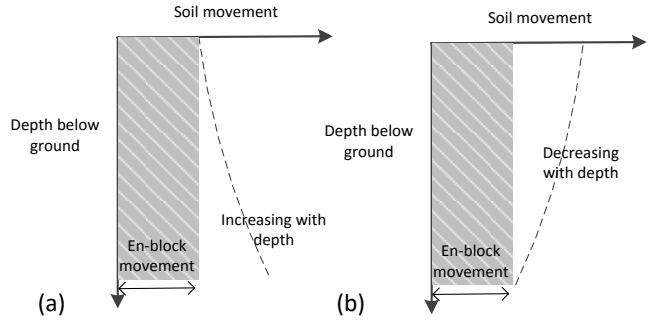

Figure 32 Separation of actual settlement into en-block movement and relative movement between the pile head and pile toe for two cases: (a) soil settlement increases with depth and (b) soil settlement decreases with depth

7.2 APPENDIX B – Derivation of the subsurface points of inflections with depth

The Gaussian settlement profile is commonly expressed as (New & O'Reily, 1991; Peck, 1969):

$$S = S_{max} \exp\left(-\frac{x^2}{2i^2}\right) \quad (7)$$

where S_{max} is the maximum settlement which occurs above the tunnel centre line, x is the horizontal distance away from the tunnel centre, i is the point of inflection or commonly referred to as the trough width parameter, which in turn is often defined using:

$$i = kz_t \quad (8)$$

where z_t is the distance between the tunnel centre and the elevation of interest. For clays, k is typically 0.5. For sub-surface settlements, Mair et al. (1993) proposed that

$$k = \frac{0.175 + 0.325(1 - z/z_0)}{1 - z/z_0} \quad (9)$$

Noting that $z_t = z - z_0$, and substituting Eq.(8) in to Eq. (9), we obtain:

$$\frac{i}{z_0} = 0.5 - 0.825\frac{z}{z_0} + 0.325\left(\frac{z}{z_0}\right)^2 \quad (10)$$

8. REFERENCES

Atkinson, J.H. (2007). The Mechanics of Soils and Foundations, Taylors & Francis, 2nd edition. pp 442.

Basile, F. (2014). Soils and Foundations. "Effects of tunnelling on pile foundations". Soils and Foundations, Vol. 54, 3,pp 280-295.

Boon, C.W. (2013). "The Distinct Element Modelling of Jointed Rock Masses: Algorithms and Their Verification". DPhil Thesis. University of Oxford.

Boon, C.W., Teh, E.H., and Ooi, L.H (2015 a). "Protection of buildings and structures within the influence of tunnelling works". International Conference and Exhibition on Tunnelling & Underground Space (ICETUS 2015), 3 – 5 March, Ooi T.A., Ooi, L.H. (Eds.), Tunnelling & Underground Space Division, The Institution of Engineers, Malaysia, pp 256-262.

Boon, C.W., Houlsby, G.T., Utili, S. (2015 b). "Designing tunnel support in jointed rock masses via the DEM". Rock Mechanics and Rock Engineering, 48(2), pp 603-632.

Boon, C.W., and Ooi, L.H. (2016): "Type II Factor of Safety: Reliability of Information from Instrumentation, Numerical Analysis, Site Investigation and Design". 19th Southeast Asian Geotechnical Conference & 2nd AGSSEA Conference (19SEAGC & 2AGSSEA) Young Geotechnical Engineers Conference, Kuala Lumpur, 30 May 2016, pp 40-45.

Burd, H.J., G.T. Houlsby, Augarde, C.E., and Gang, L. (2000). "Modelling tunnelling-induced settlement of masonry buildings". Proc. Instn. Civ. Engrs. Geotech. Engng, Vol. 143, Jan, pp 17-29.

Chang, M.F., and Broms, B.B. (1991). "Design of bored piles in residual soils based on field-performance data". Canadian Geotechnical Journal, 28(2), pp 200-209.

Chen, L.T., Poulos, H.G. & Loganathan, N. (1999). "Pile responses caused by tunnelling". J. Geotech. Geoenv. Engng ASCE, Vol. 125, 3, pp 207-215.

Chen, L.T., Poulos, H.G., and Loganathan, N. (2000). "Approximate design charts for piles adjacent to tunnelling operations". Proceedings GEOENG – 2000.

Coyle, H. M. and Reese, L. C. (1966). "Load transfer for axially loaded piles in clay". Journal of Soil Mechanics and Foundations Division, ASCE, vol. 92, SM2, pp. 1-26.\

Gens, A., Mariano, D., Yubero, M.T. (2012). "EPB tunnelling in deltaic deposits: Observations of ground movements". In: Proceedings of the 7th International Symposium on Geotechnical Aspects of Underground Construction in Soft Ground, Viggiani G. (Ed.), 17-19 May 2011, Roma, Italy, Taylor & Francis Group, pp 987-994.

Jacobsz, S.W., Standing, J.R., Mair, R.J., Hagiwara, T., and Sugiyama, T. (2004). "Centrifuge modelling of tunnelling near driven piles. Soils and Foundations", Vol. 44, 1, pp 49-56.

Kaalberg, F.J., Teunissen, E.H., van Tol, A.F. and Bosch, J.W. (2006). "Dutch research on the impact of shield tunnelling on pile foundations". In: Proceedings of the 5th International Symposium on Geotechnical Aspects of Underground

Construction in Soft Ground, Amsterdam, the Netherlands, 15-17 June 2005, pp 123-133. Edited by E. A. Kwast , K. J. Bakker , W. Broere , and A. Bezuijen.

Khoo, C.M., Ooi, T.A., Ng, S.W.F., and Feng, Q.Y. (2015). "An innovative approach of mined adit design and construction for removal of existing piles". International Conference and Exhibition on Tunnelling & Underground Space (ICETUS 2015), 3 – 5 March, Ooi T.A., Ooi, L.H. (Eds.), Tunnelling & Underground Space Division, The Institution of Engineers, Malaysia, pp268-271.

Kok, Y. L., (2006). Investigating the mechanical behaviour of two residual soils from Malaysia. Ph.D. thesis. University of Cambridge. 1-309.

Kraft, L.M, Ray, R.P., and Kagawa, T. (1981). "Theoretical t-z curves". J. Geotechnical Engineering Division, ASCE, Vol. 107 (11), pp 1543-1560.

Lee, R.G., Rowe, R.K., and Lo, K.Y., (1992). "Subsidence owing to tunnelling I: Estimating the gap parameter". Canadian Geotechnical Journal, 29, 929-940.

Lee, G., and Ng, C. (2005). "Effects of Advancing Open Face Tunneling on an Existing Loaded Pile". J. Geotech. Geoenviron. Eng., Vol. 131, No. 2, pp 193-201.

Lee, C.-J. and Chiang, K.-H. (2007). "Responses of single piles to tunneling-induced soil movements in sandy ground". Canadian Geotechnical Journal, Vol. 44, 10, pp 1224-1241.

Loganathan, N. and Poulos, H.G., 1998. "Analytical prediction for tunneling-induced ground movements in clays". J. Geotech. and Geoenvir. Eng. 124(9), 846-856.

Mak, W.K., Cheah, F., and Ishak, A. (2015). "Challenges in assessment of existing old road bridge due to tunnelling works". 9th International Symposium on Field Measurements in Geomechanics (FMGM), 9-11 September, Dight, P. (Eds.), Sydney, Australia, Australian Centre for Geomechanics, pp 292-297.

Mair, R.J., Taylor, R.N., and Bracegirdle, A. (1993). "Subsurface settlement profiles above tunnels in clays". Géotechnique, 43(2), pp 315-320.

Marshall, A.M. (2012). "Tunnel-pile interaction analysis using cavity expansion methods". Journal of Geotechnical and Geoenvironmental Engineering, ASCE, Vol. 138, pp 1237-1246.

Mroueh, H., and Shahrour, I. (2002). "Three-dimensional finite element analysis of the interaction between tunneling and pile foundations". Numerical and Analytical Methods in Geomechanics, Vol. 26, 3, pp. 217-230.

New, B.M., and O'Reilly, M.P, (1991). "Tunnelling-induced Ground Movements: predicting their magnitude and effects". 4th International Conference on Ground Movements and Structures, Cardiff, invited review paper, pp. 691–697.

Nithiaraj, R., Ting, W.H., and Balasubramaniam, A.S. (1996). "Strength parameters of residual soils and application to stability analysis of anchored slopes". Geotechnical Engineering, 27, 55-81.

Ong, D.E.L. (2008). "Finite element analysis in geotechnical engineering – part 2: an indispensable tool or a mysterious black box". Jurutera, September 2008, pp 28-31.

Ong, V.C.W. (2015). "Challenges of Construction of Twin Bored MRT Tunnels in Singapore", GeoSmart Asia 2015.

Ong, V.C.W. & Ng, D.C.C. (2014). "Overview of Design & Construction of Deep Excavation & Tunnelling Projects in Singapore", Seminar organized by the Tunnelling & Underground Space Technical Division (TUSTC), The Institution of Engineers Malaysia (IEM), 26 July 2014.

Ooi, T.A., and Khoo, C.M. (2016). "Instrumented Load Test on Bored Cast-in-situ Pile in Kenny Hill Formation". 19th Southeast Asian Geotechnical Conference & 2nd AGSSEA Conference (19SEAGC & 2AGSSEA), Kuala Lumpur, 31 May-3 June 2016, pp 853-859.

Peck, R.B. (1969). "Deep excavations and tunnelling in soft ground". Proc. 7th Int. Conf. Soil Mechanics and Foundation Engineering, Mexico City, State of the Art Volume, 225-290.

Poulos, H.G., Mattes, N.S. (1971). "Settlement and load distribution of pile groups". Australian Geomechanics Journal, G1, pp 18-28.

Poulos, H.G. (2005). "Pile behavior – consequences of geological and construction imperfections". Journal of Geotechnical and Geoenvironmental Engineering, ASCE, Vol. 131, 5, pp 538-563.

Poulos, H.G., and Davis, E.H. (1981). "Pile foundation analysis and design". John Wiley and Sons, pp. 410.

Poulos, H.G., and Deng, W. (2004). "An investigation on tunnelling-induced reduction of pile geotechnical capacity". Proc. 9th Australia-New Zealand Conf. On Geomechanics, Auckland, Vol. 1, 116-122.

Randolph, M. F., and Wroth, C. P. (1978). "Analysis of deformation of vertically loaded piles". Journal of the Geotechnical Engineering Division, American Society of Civil Engineers, Proceedings Paper 14262/Vol 104(GT12), pp 1465-1488.

Sadek M, and Shahrour I. (2004). "A three dimensional embedded beam element for reinforced geomaterials". Int J Numer Anal Methods Geomech; 28(9): 931–46.

Schanz, T., Vermeer, P.A., and Bonnier, P.G. (1999). "Formulation and verification of the Hardening-Soil Model". In Beyond 2000 in Computational Geotechnics. R.B.J. Balkema Brinkgreve, Rotterdam. 281–290.

Seed, H. B., and Reese, L. C. (1957). "The action of soft clay along friction piles". Transactions, American Society ofCivil Engineers, Vol 122, pp 1-26.

The European Federation of Foundation Contractors (2015). "Game Changer". European Foundations: Winter 2015, Magazine of the EFFC, pp. 17-22.

Thewes, M., and Budach C. (2009). "Grouting of the annular gap in shield tunnelling – An important factor for minimisation of settlements and production performance", ITA-AITES World Tunnel Congress 2009, Safe Tunnelling for the City and Environment, 23-28 May.

Wong, J., and Muhinder, S. (1996). "Some engineering properties of weathered Kenny Hill Formation in Kuala Lumpur", Proceedings of the 12th South East Asian Geotechnical Conference, 1, pp179-187.